Clays and Clay Minerals, Vol. 56, No. 4, 397–403, 2008.

INFLUENCE OF Mn(III) AVAILABILITY ON THE PHASE TRANSFORMATION FROM LAYERED BUSERITE TO TUNNEL-STRUCTURED TODOROKITE

HAOJIE CUI[1], XIANGWEN LIU[2], WENFENG TAN[1], XIONGHAN FENG[1,*], FAN LIU[1], AND HUADA DANIEL RUAN[3]

[1]Key Laboratory of Subtropical Agricultural Resources and Environment, Ministry of Agriculture, Huazhong Agricultural University, Wuhan 430070, People's Republic of China
[2]China University of Geosciences, Wuhan 430074, People's Republic of China
[3] Environmental Science Program, Division of Science and Technology, United International College, Beijing Normal University-Hong Kong Baptist University, Zhuhai 519085, People's Republic of China

Abstract—Todorokite is a common Mn oxide mineral in terrestrial and ocean-floor environments, and it is commonly synthesized from layered Na-buserite. Pyrophosphate, which is known to form strong complexes with Mn(III) at a pH range of 1−8, was added to a suspension of Na-buserite in order to sequester the available Mn(III) in Na-buserite. No Mn(III)-pyrophosphate complex was formed in solution at pH 10, and the treated Na-buserites were converted completely to todorokite. Significant transformation reductions were observed when Na-buserite was treated with pyrophosphate solution at pH 7. The presence of Mn(III) within the MnO_6 octahedral sheets of Na-buserite is critical for the transformation from layered buserite to tunnel-structured todorokite at atmospheric pressure. At lower pH, two effects are combined to reduce the amount of Mn(III) in the layers: (1) the complexing power of pyrophosphate is increased; and (2) the transformation from Na-buserite to H-birnessite, which is concomitant with the migration of Mn(III) from layers to the interlayer, and the partial disproportionation of Mn(III). The results showed that Mn(III) played a key role in the transformation of layered Na-buserite to tunnel-structured todorokite at atmospheric pressure.

Key Words—Buserite, Mn Oxide, Todorokite, Transformation, Refluxing.

INTRODUCTION

Todorokites are commonly found in soil, terrestrial Mn ore deposits, and marine Mn nodules (Turner *et al*., 1982; Golden *et al*., 1986; Shen *et al*., 1993; Post, 1999). Todorokites have been studied extensively because of their particular properties which make them suitable for use as ion sieves, molecular sieves, catalysts, and cathode materials for Li batteries (Shen *et al*., 1993; Post, 1999; Al-Sagheer and Zaki, 2004; Kumagai *et al*., 2005). Since the discovery of todorokite in 1934 in the Japanese mine, Todoroki, its synthetic counterpart has been used to study its structure, properties, and origin. The most common synthetic route to create todorokite is hydrothermal treatment or a refluxing process of metal-buserite (*Me*-buserite), the layer-structured precursor of todorokite (Golden *et al*., 1987; Shen *et al*., 1994; Luo *et al*., 1999; Feng *et al*., 2004a; Cui *et al*., 2006). Recently, Bodeï *et al.* (2007) reported the formation of todorokite from vernadite in Ni-rich hemipelagic sediments. Almost all synthetic routes to todorokite differ only in the initial synthesis of Na-buserite or in the treatment methods of *Me*-buserite, *e.g.* Na-buserite exchanged with different metal ions as an interlayer ion.

According to recent reports in the literature, Na-buserite is a layered Mn oxide formed by edge-shared MnO_6 octahedra with mixed Mn(IV) and Mn(III) octahedra (Drits *et al*., 1997; Silvester *et al*., 1997; Lanson *et al*., 2002a). Todorokite has a 3×3 tunnel structure with corner-sharing triple chains of MnO_6 octahedra, and the Mn(III) occupy large octahedral sites at the edges of the triple chains (Post *et al*., 2003). Experimental results revealed that many parameters seem to influence the phase transformation from Na-buserite to todorokite, *e.g.* the types and sizes of the guest cations, the amount of water molecules in adjacent layers, and the sub-structure of MnO_6 layers. Although details of the phase transformation from layer to tunnel structure are still unclear, the migration of Mn(III) may play critical roles in forming the tunnel structure (Liu *et al*., 2002; Feng *et al*., 2004a; Liu *et al*., 2005). The amount of migration and the disproportionation of Mn(III) in the layer of Na-buserite depends mainly on the pH of the solution (Silvester *et al*., 1997; Lanson *et al*., 2000). The solution pH of various metal salts, which depends on the hydrolysis constant of metal ions, governs the amount of migration and disproportionation of Mn(III) from the MnO_6 layers when Na-buserite is exchanged with other divalent metals to form *Me*-buserites. At a high solution pH, such as a $MgCl_2$ solution where Na is exchanged with Mg to form Mg-buserite, almost no Mn(III) migrates into the interlayer from MnO_6 layers or disproportionates to Mn(II) and Mn(IV), and no Mn(II) is released into the solution. Therefore, Mg-buserite can easily convert to todorokite at atmospheric pressure. However, in a low-pH solution,

* E-mail address of corresponding author:
fxh73@mail.hzau.edu.cn
DOI: 10.1346/CCMN.2008.0560401

such as a $CuCl_2$ solution where Na is exchanged with Cu to form Cu-buserite, more Mn(III) migrates into the interlayer and/or disproportionates to Mn(II) and Mn(IV), forming layer vacancies. The Cu^{2+} forms an interlayer complex above the vacancies by replacing Mn^{2+} or H^+ (Lanson *et al.*, 2000; Manceau *et al.*, 2002). Todorokite formation was difficult after refluxing Cu-buserite at atmospheric pressure (Cui *et al.*, 2005), which suggests that Mn(III) plays a key role in the transformation from Na-buserite to todorokite.

Dissolved Mn(III) is unstable in aquatic environments, and can disproportionate to Mn(II) and Mn(IV). However, soluble Mn(III) can be stabilized with organic and inorganic ligands to prevent disproportionation (Klewicki and Morgan, 1998). Pyrophosphate, a particularly good chelating agent, was shown to form strong complexes with Mn(III), and the Mn(III)-pyrophosphate complexes formed were clear with a red tint and easily measured by ultraviolet-visible spectrophotometry (Kostka *et al.*, 1995; Klewicki and Morgan, 1998; Nguyen *et al.*, 2002; Webb *et al.*, 2005). Mn(III) availability for phase transformation from layered to tunnel-structured Mn oxide can be predicted by the Mn(III) complexation with pyrophosphate. Evidence is presented here that strongly links Mn(III) availability to the transformation from layered Na-buserite to todorokite and which delineates the mechanisms of transformation from layered to tunnel-structured Mn oxides.

EXPERIMENTAL

Preparation of Na-buserite

Na-buserite was prepared as follows: 250 mL of 5.5 M NaOH solution (<273 K) was added quickly to 200 mL of 0.5 M $MnCl_2$ solution to form a white $Mn(OH)_2$ precipitate and O_2 was bubbled immediately at a rate of 1.5 L/min. After oxidation for 5 h, the black precipitate was washed with distilled deionized water (DDW) until the pH was ~7 (Feng *et al.*, 2004b).

Treatments of Na-buserite using $Na_4P_2O_7$ solutions

Two grams of purified Na-buserite (still wet) was dispersed in 200 mL of 0.05 M $Na_4P_2O_7$ at pH 7 and pH 10. After stirring at mid-speed for 12 h, the suspensions were centrifuged and the supernatants were used to detect the Mn(III)-pyrophosphate complexes. The solids were washed 3−5 times with DDW.

Two grams of purified Na-buserite (still wet) was dispersed in 200 mL of 0, 0.01, 0.025, 0.05, or 0.10 M $Na_4P_2O_7$ at pH 7. After stirring at mid-speed for 12 h, the suspensions were treated with the same procedures as above.

Two grams of purified Na-buserite (still wet) was dispersed in 200 mL of 0.05 M $Na_4P_2O_7$ at pH 7 and stirred at mid-speed for 1, 2, 4, 8, 12, and 24 h. The suspensions were treated with the same procedures as above.

Ion-exchange of Na-buserite and subsequent conversion to todorokite

Two Na-buserite samples, one untreated and the other treated with $Na_4P_2O_7$, were dispersed in different 400 mL solutions of 0.5 M $MgCl_2$. After stirring at mid-speed for 12 h, the suspensions were centrifuged and the solids were washed 3−5 times with DDW. The products were dispersed in 400 mL of DDW, then the suspensions were transferred to flasks and refluxed (373 K) with stirring for 12 h at atmospheric pressure. The refluxed solutions were centrifuged and the products were washed 3−5 times with DDW and dried. The refluxing time was extended to 48 h for the Na-buserite treated with 0.05 M $Na_4P_2O_7$ at pH 7; the intermediate products at refluxing times of 12, 24, and 48 h were used to characterize the effects of refluxing time on the formation of todorokite.

Methods of analysis

Measure of Mn(III)-pyrophosphate complex. Two grams of manganite (AOS = 3.05) was dispersed in 100 mL of $Na_4P_2O_7$ solution at pH 6. The suspension was stirred vigorously for 12 h at room temperature and then centrifuged at 22,400 g for 10 min in a Beckman Superspeed refrigerated centrifuge. The supernatant liquid was stored to serve as standard stock solution.

Ten milliliters of the manganite stock solution was mixed with 5 mL of 0.5 M $H_2C_2O_4$ and 10 mL of 1 mol/L H_2SO_4 to reduce all of the Mn(III) to Mn(II). The excess $C_2O_4^{2-}$ was determined by back-titration at 348 K with standardized 0.02555 mol/L $KMnO_4$ solution. Three duplicate measurements were taken and averaged. Additionally, a blank control group was prepared without manganite. Then, the concentration of Mn in the Mn(III) standard stock solution was obtained. A calibration curve was obtained using a Mn(III) standard stock solution diluted by factors of 4, 5, 10, 20, and 40, each adjusted to pH 8. At pH 8, the pyrophosphate existed mainly as $HP_2O_7^{3-}$ in the solution. Then, the concentration of the Mn(III) complex was determined by visible spectrophotometry (Rayleigh vis-7220 model) at 482 nm. A 0.05 mol/L solution of sodium pyrophosphate at pH 8 served as the blank for absorbance measurements.

The concentration of Mn(III) in the supernatant solution was measured from the original Na-buserite treated with $Na_4P_2O_7$ at pH 7 and 10. The supernatant solution was adjusted to pH 8, and then filtered through a 0.45 μm membrane. The absorbance of the filtrate was determined by visible spectrophotometry at 482 nm. The amount of Mn(III) in the filtrate was obtained from the above calibration curve.

X-ray diffraction analysis. X-ray diffraction (XRD) was carried out at ambient temperature, using a Rigaku D/Max-3B diffractometer with monochromated FeKα radiation. The diffractometer was operated at a tube voltage of 40 kV, a current of 20 mA, and a step

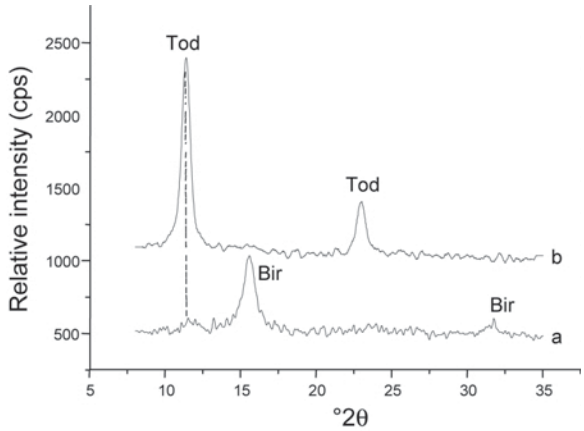

Figure 1. XRD patterns of reflux products of Na-buserites treated with 0.05 M $Na_4P_2O_7$ solution at (a) pH 7, and (b) pH10; Tod – todorokite, Bir – birnessite

scanning rate of 0.02º2θ per 0.5 s. Both buserites and todorokites have basal spacings of 1 nm (1 nm manganate). After heating or dehydrating, the buserites became unstable and transformed to 0.7 nm manganate. However, todorokite is relatively stable at high temperature. To eliminate the interference of diffraction peaks of buserite during the identification of todorokite, the oriented samples were spread onto the glass slide for the refluxed products heated at 413 K for 10 h before XRD analysis (Feng *et al.*, 2004a).

Transmission electron microscopy measurement. The samples were crushed gently to powder, dispersed in absolute alcohol, sonified, deposited on a holey copper grid, and then air dried. Transmission electron microscopy (TEM) images and electron diffraction patterns were obtained using a Philips-CM12 TEM at an accelerating voltage of 120 kV.

RESULTS

Effect of pH in $Na_4P_2O_7$ solutions on the phase transformation from Na-buserite to todorokite

Treatment of Na-buserite with 0.05 M $Na_4P_2O_7$ solution at pH 7 produced a very weak XRD peak (Figure 1) of todorokite and a strong diffraction peak of birnessite, indicating that a small amount of Na-buserite was converted to todorokite. When the pH value of $Na_4P_2O_7$ solution was adjusted to 10, the diffraction peak of birnessite disappeared, and the diffraction peak of todorokite became much stronger, which indicates that Na-buserite had been completely converted to todorokite (Figure 1). Moreover, the typical characteristics of todorokite were observed from the TEM bright-field images (Figure 2a) and the electron diffraction (ED) patterns (Figure 2b). The formation of todorokite was not affected by the Na-buserite treated with 0.05 M $Na_4P_2O_7$ solutions at pH 10.

Effect of $Na_4P_2O_7$ concentration at pH 7 on the phase transformation from Na-buserite to todorokite

The XRD patterns of the reflux products of Na-buserites treated with different concentrations of $Na_4P_2O_7$ solutions at pH 7 (Figure 3) revealed that when synthetic Na-buserite was used as the precursor for the synthesis of todorokite, only the characteristic peaks of todorokite appeared in the XRD pattern. The XRD peaks indicate that Na-buserite can be converted completely to todorokite by the refluxing method at atmospheric pressure (Figure 3a). Na-buserite treated with 0.01 M $Na_4P_2O_7$ solution at pH 7 produced a weak diffraction peak of birnessite, and the intensity of the todorokite peaks became weaker, indicating that less Na-buserite was converted to todorokite and more Na-buserite was dehydrated to form birnessite (Figure 3b).

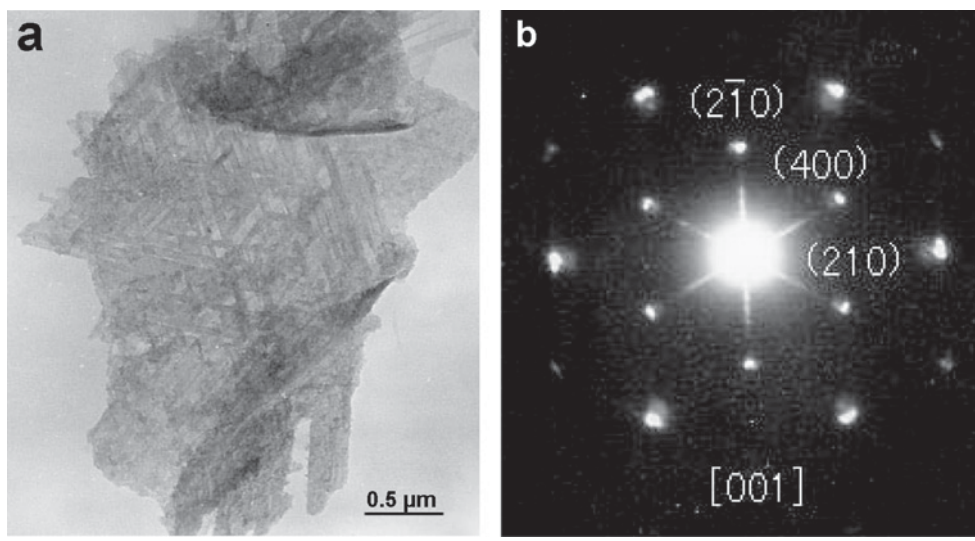

Figure 2. TEM image (a) and ED pattern (b) of reflux product of Na-buserite treated with 0.5 M $Na_4P_2O_7$ solution at pH 10.

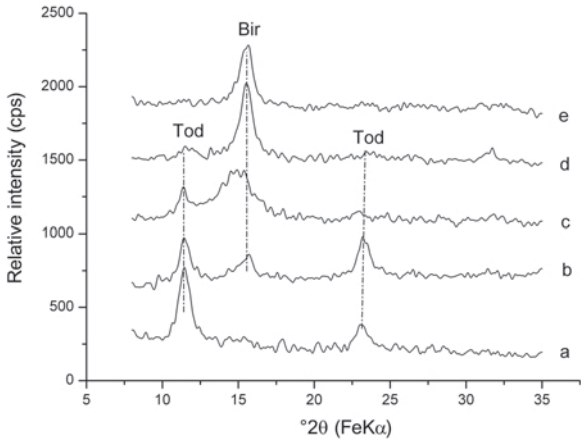

Figure 3. XRD patterns of refluxed products of Na-buserite treated with different concentrations of $Na_4P_2O_7$ solutions at pH 7: (a) 0 M, (b) 0.01 M, (c) 0.025 M, (d) 0.05 M, and (e) 0.10 M.

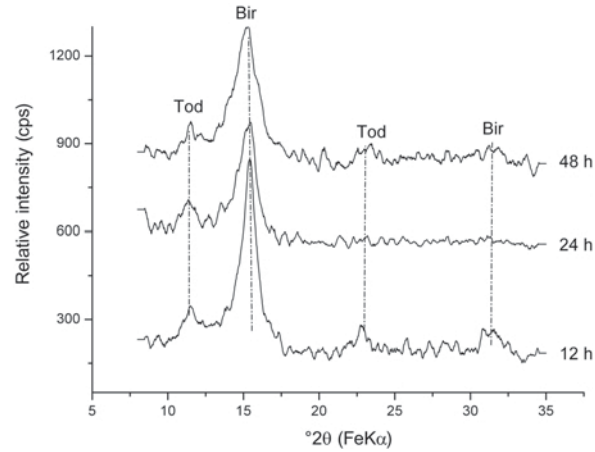

Figure 5. XRD patterns of intermediate products at different stages of reflux with Na-buserite treated with 0.05 M $Na_4P_2O_7$ at pH 7.

The intensity of the todorokite peaks decreased while those of birnessite increased gradually during the increase of $Na_4P_2O_7$ in solution from 0.01 to 0.05 M (Figure 3b–d). When Na-buserite was treated with 0.10 M $Na_4P_2O_7$ solution at pH 7, the diffraction peaks of todorokite disappeared, leaving only the characteristic peaks of birnessite (Figure 3e). This indicates that Na-buserite could not be converted to todorokite after equilibration in 0.10 M $Na_4P_2O_7$ solution at pH 7.

Effect of $Na_4P_2O_7$ treatment time on phase transformation from Na-buserite to todorokite

Weak diffraction peaks of birnessite appeared in the XRD patterns of reflux products of Na-buserites treated with 0.05 M $Na_4P_2O_7$ solution at pH 7 for 1 h (Figure 4), showing that only a small amount of Na-buserite could not be converted to todorokite. With a treatment time of 2 h, the intensity of the characteristic peaks of todorokite decreased, while the intensity of the characteristic peaks of birnessite increased, indicating that a large proportion of Na-buserite could not transform to todorokite. The intensity of the characteristic peaks of todorokite became weaker and those of birnessite increased further when the treatment time was prolonged from 4 to 8 h, indicating a decreasing amount of todorokite production. After treating Na-buserite with 0.05 M $Na_4P_2O_7$ solution at pH 7 for 12–24 h, the diffraction peaks of todorokite disappeared. In contrast, the intensity of characteristic peaks of birnessite became stronger, indicating that Na-buserites did not transform to todorokite but birnessite.

Effect of reflux time on the phase transformation from Na-buserite to todorokite

Cui *et al.* (2005) showed that the temperature and time of reflux reaction significantly influenced the transformation from Na-buserite to todorokite at atmospheric pressure. The XRD patterns of intermediate products at different stages of reflux with Na-buserite

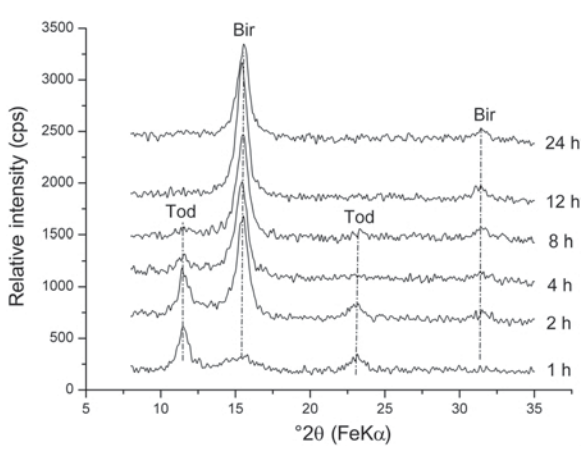

Figure 4. XRD patterns of reflux products of Na-buserites treated with 0.05 M $Na_4P_2O_7$ at pH 7 at different time intervals.

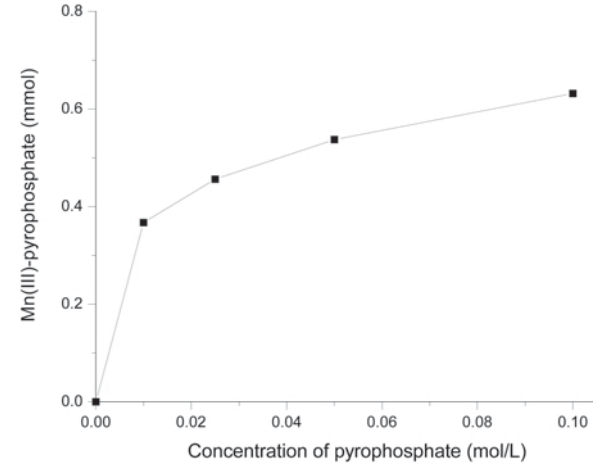

Figure 6. Formation of Mn(III)-pyrophosphate complex in different concentrations of pyrophosphate at pH 7.

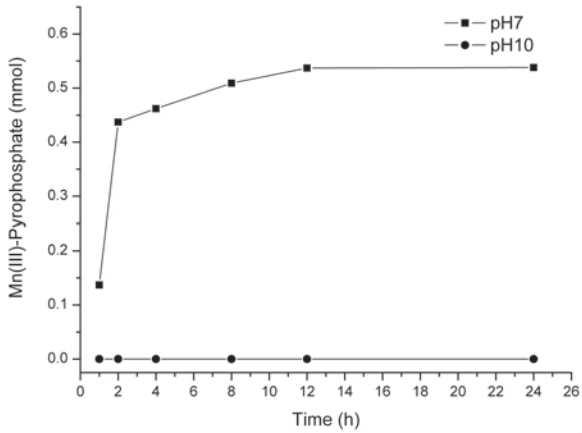

Figure 7. Amount of Mn(III)-pyrophosphate *vs.* treatment time of Na-buserite treated with 0.05 M pyrophosphate solution at pH 7 and pH 10.

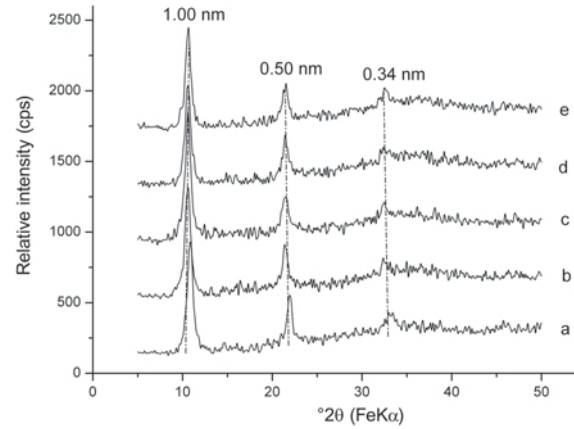

Figure 8. XRD patterns of Na-buserite treated with different concentrations of $Na_4P_2O_7$ at pH 7: (a) 0 M; (b) 0.01 M; (c) 0.025 M; (d) 0.05 M; (e) 0.10 M

treated with 0.05 M $Na_4P_2O_7$ at pH 7 are shown in Figure 5. A weak diffraction peak of todorokite and a strong diffraction peak of birnessite in the XRD patterns of the intermediate products obtained after 12 h of reflux indicate that very small amounts of Na-buserite had been converted into todorokite. After 24 h of reflux, the intensity of the characteristic peaks of todorokite increased slightly whereas those of birnessite decreased. The intensity of the todorokite and birnessite peaks did not increase further when the refluxing time was prolonged to 48 h. Cui *et al*. (2005) showed that the rate of formation of todorokite increased with prolonged reflux time at atmospheric pressure. However, the lack of peak augmentation demonstrates that no more todorokite was obtained by prolonging the refluxing time. This shows that the transformation from Na-buserite to todorokite is governed mainly by $Na_4P_2O_7$ solution treatment at pH 7 in the present work.

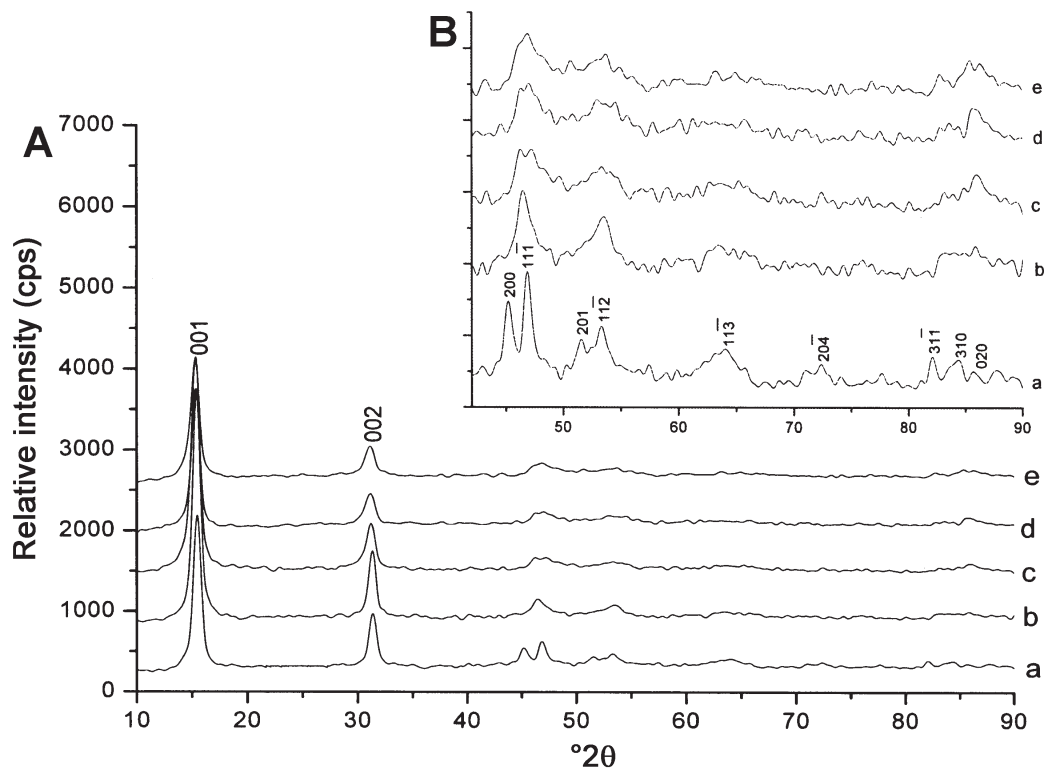

Figure 9. Powder XRD patterns of Na-buserite after conversion to birnessite by drying and treating with different concentrations of $Na_4P_2O_7$ at pH 7: (a) 0 M; (b) 0.01 M; (c) 0.025 M; (d) 0.05 M; (e) 0.10 M (A: 10−90°2θ; B: 40−90°2θ).

DISCUSSION AND CONCLUSIONS

Mn(III) was shown to form a stable complex with pyrophosphate from pH 1 to 8, and the Mn(III)-pyrophosphate complexes formed were clear with a red tint (Kostka *et al.*, 1995; Klewicki and Morgan, 1998). When Na-buserite was treated with pyrophosphate solutions at pH 7, a red Mn(III)-pyrophosphate complex was observed in the treated solutions, indicating that Mn(III) began to migrate into solution from MnO_6 layers because of chelation with pyrophosphate. The amount of Mn(III)-pyrophosphate increased with the increase in pyrophosphate concentration and in treatment time (Figures 6 and 7). After treating Na-buserite with different concentrations of $Na_4P_2O_7$ solutions at pH 7, all XRD patterns of the products were similar to that of Na-buserite (Figure 8) except the 20*l* and 11*l* reflections over the 40−90º2θ FeKα range, where XRD patterns of Na-birnessite (buserite converted into birnessite by drying) became broad or disappeared after treating with $Na_4P_2O_7$ solutions (Figure 9). These 20*l* and 11*l* reflections are the most sensitive structural parameters of layered minerals (Lanson *et al.*, 2000, 2002b), so the migration of Mn(III) from MnO_6 layers may have altered the sub-structure of the layered Na-buserite.

During the transformation process, some of the Mn(III) octahedra from the layers of the precursors may have migrated into the interlayer region; this migration was followed by the rearrangement of Mn to form the wall of a tunnel. The amount of Mn(III) which migrated from the layer to interlayer during the course of transformation may govern the formation of todorokite at atmospheric pressure. When Na-buserite was treated with pyrophosphate solutions at pH 7, two effects are combined to reduce the amount of Mn(III) within the octahedral layers: (1) Mn(III) migrated from MnO_6 layers and formed complexes with pyrophosphate in solution; and (2) some Na-buserite may convert to H-birnessite, which includes the migration of Mn(III) from octahedral layers to the interlayer and the partial disproportionation of Mn(III). As a result, the ability of Mn(III) to assist the formation of tunnel structures decreased and the transformation from Na-buserite to todorokite was restricted to some extent. The amount of todorokite formed decreased with increase in the Mn(III)-pyrophosphate complex (Figures 3, 4). However, when Na-buserite was treated with $Na_4P_2O_7$ solutions at pH 10, the pyrophosphate could not complex Mn(III) and no red color arose (Figure 7). Moreover, the transformation from Na-buserite to H-birnessite would be ruled out at the higher pH. Under such a reaction condition, Mn(III) still remained in the layers of Na-buserite, and thus the Na-buserite can be completely converted to todorokite by the refluxing method at atmospheric pressure (Figure 1). These experiments demonstrate the importance of Mn(III) availability for the transformation from layered to tunnel-structured Mn oxide at atmospheric pressure .

ACKNOWLEDGMENTS

The authors gratefully acknowledge Associate Editor, Bruno Lanson, and two anonymous reviewers for their helpful comments and suggestions. They are grateful also to Matthew Siebecker for his kind help in reviewing the final draft and improving the English. The National Natural Science Foundation of China (grant numbers 40403009 and 40471070) and the Foundation for the Author of National Excellent Doctoral Dissertation of China (No. 200767) are thanked for financial support of this research.

REFERENCES

Al-Sagheer, F.A. and Zaki, M.L. (2004) Synthesis and surface characterization of todorokite-type microporous manganese oxides: implications for shape-selective oxidation catalysts. *Microporous and Mesoporous Materials*, **67,** 43−52.

Bodeï, S., Manceau, A., Geoffroy, N., Baronnet, A., and Buatier, M. (2007) Formation of todorokite from vernadite in Ni-rich hemipelagic sediments. *Geochimica et Cosmochimica Acta*, **71**, 5698−5716.

Cui, H.J., Feng, X.H., Liu, F., Tan, W.F., and He, J.Z. (2005) Factors governing formation of todorokite at atmospheric pressure. *Science in China Series D*, **48**, 1678−1689.

Cui, H.J., Feng, X.H., He, J.Z., Tan, W.F., and Liu, F. (2006) Effects of reaction conditions on the formation of todorokite at atmospheric pressure. *Clays and Clay Minerals*, **54**, 605−615.

Drits, V.A., Silvester, E., Gorshkov, A.I., and Manceau, A. (1997) Structure of synthetic monoclinic Na-rich birnessite and hexagonal birnessite: I. Results from X-ray diffraction and selected-area electron diffraction. *American Mineralogist*, **82**, 946−961.

Feng, X.H., Tan, W.F., Liu, F., Wang, J.B., and Ruan, H.D. (2004a) Synthesis of todorokite at atmospheric pressure. *Chemistry of Materials*, **16**, 4330−4336.

Feng, X.H., Liu, F., Tan, W.F., and Liu, X.W. (2004b) Synthesis of birnessite from the oxidation of Mn^{2+} by O_2 in alkali medium: Effects of synthesis conditions. *Clays and Clay Minerals*, **52**, 240−250.

Golden, D.C., Chen, C.C., and Dixon, J.B. (1986) Synthesis of todorokite. *Science*, **231**, 717−719.

Golden, D.C., Chen, C.C., and Dixon, J.B. (1987) Transformation of birnessite to buserite, todorokite, and manganite under mild hydrothermal treatment. *Clays and Clay Minerals*, **35**, 271−280.

Klewicki, J.K. and Morgan, J.J. (1998) Kinetic behavior of Mn(III) complexes of pyrophosphate, EDTA, and citrate. *Environmental Science & Technology*, **32**, 2916−2922.

Kostka, J.E., Luther, G.W., III, and Nealson, K.H. (1995) Chemical and biological reduction of Mn(III)-pyrophosphate complexes: Potential importance of dissolved Mn(III) as an environmental oxidant. *Geochimica et Cosmochimica Acta*, **59**, 885−894.

Kumagai, N., Komaba, S., Abe, K., and Yashiro, H. (2005) Synthesis of metal-doped todorokite-type MnO_2 and its cathode characteristics for rechargeable lithium batteries. *Journal of Power Sources*, **146**, 310−314.

Lanson, B., Drits, V.A., Silvester, E., and Manceau, A. (2000) Structure of H-exchanged hexagonal birnessite and its mechanism of formation from Na-rich monoclinic buserite at low pH. *American Mineralogist*, **85**, 826−838.

Lanson, B., Drits, V.A., Feng, Q., and Manceau, A. (2002a) Structure of synthetic Na-birnessite: Evidence for a triclinic one-layer unit cell. *American Mineralogist*, **87**, 1662−1671.

Lanson, B., Drits, V., Gaillot, A., Silvester, E., Plançon, A., and Manceau, A. (2002b) Structure of heavy-metal sorbed

birnessite: Part 1. Results from X-ray diffraction. *American Mineralogist*, **87**, 1631–1645.

Liu, J., Cai, J., Son, Y. C., Gao, Q., Suib, S.L., and Aindow, M. (2002) Magnesium manganese oxide nanoribbons: Synthesis, characterization, and catalytic application. *Journal of Physical Chemistry B*, **106**, 9761–9768.

Liu, Z., Kang, L., Ooi, K., Makita, Y., and Feng, Q. (2005) Studies on the formation of todorokite-type manganese oxide with different crystalline birnessites by Mg^{2+}-templating reaction. *Journal of Colloid and Interface Science*, **285**, 239–246.

Luo, J., Zhang, Q., Huang, A., Giraldo, O., and Suib, S.L. (1999) Double-aging method for preparation of stabilized Na-buserite and transformations to todorokites incorporated with various metals. *Inorganic Chemistry*, **38**, 6106–6113.

Manceau, A., Lanson, B., and Drits, V. (2002) Structure of heavy metal sorbed birnessite. Part III: Results from powder and polarized extended X-ray absorption fine structure spectroscopy. *Geochimica et Cosmochimica Acta*, **66**, 2639–2663.

Nguyen, M., Quemard, A., Broussy, S., Bernadou, J., and Meunier, B. (2002) Mn(III) pyrophosphate as an efficient tool for studying the mode of action of Isoniazid on the InhA protein of Mycobacterium tuberculosis. *Antimicrobial Agents and Chemotherapy*, **46**, 2137–2144.

Post, J.E. (1999) Manganese oxide minerals: Crystal structures and economic and environmental significance. *Proceedings of the National Academy of Sciences of the United States of America*, **96**, 3447–3454

Post, J.E., Heaney, P.J., and Hanson, J. (2003) Synchrotron X-ray diffraction study of the structure and dehydration behavior of todorokite. *American Mineralogist*, **88**, 142–150.

Shen, Y.F., Zerger, R.P., DeGuzman, R.N., Suib, S.L., McCurdy, L., Potter, D.I., and O'Young, C.L. (1993) Manganese oxide octahedral molecular sieves: Preparation, characterization, and applications. *Science*, **260**, 511–515.

Shen, Y.F., Suib, S.L., and O'Young, C.L. (1994) Effects of inorganic cation templates on octahedral molecular sieves of manganese oxide. *Journal of the American Chemical Society*, **116**, 11020–11029.

Silvester, E., Manceau, A., and Drits, V.A. (1997) Structure of synthetic monoclinic Na-rich birnessite and hexagonal birnessite: II. Results from chemical studies and EXAFS spectroscopy. *American Mineralogist*, **82**, 962–978.

Turner, S., Siegel, M.D., and Buseck, P.R. (1982) Structural features of todorokite intergrowths in manganese nodules. *Nature*, **296**, 841–842.

Webb, S.M., Dick, G.J., Bargar, J.R., and Tebo, B.M. (2005) Evidence for the presence of Mn(III) intermediates in the bacterial oxidation of Mn((II). *Proceedings of the National Academy of Sciences of the United States of America*, **102**, 5558–5563.

(*Received 17 October 2007; revised 1 May 2008; Ms. 0092; A.E. B. Lanson*)